Molecular Therapy
Nucleic Acids
Original Article

5′-tiRNA-Cys-GCA regulates VSMC proliferation and phenotypic transition by targeting STAT4 in aortic dissection

Tingyu Zong,[1,7] Yanyan Yang,[2,7] Xiaotong Lin,[3] Shaoyan Jiang,[4] Hui Zhao,[5] Meixin Liu,[1] Yuanyuan Meng,[1] Yong Li,[1] Liang Zhao,[1] Guozhang Tang,[1] Kun Gong,[1] Zhibin Wang,[1] and Tao Yu[1,6]

[1]Department of Cardiac Ultrasound, The Affiliated Hospital of Qingdao University, No. 16 Jiangsu Road, Qingdao 266000, People's Republic of China; [2]Department of Immunology, Basic Medicine School, Qingdao University, Qingdao 266071, People's Republic of China; [3]Department of Respiratory Medicine, Qingdao Municipal Hospital, Qingdao 266011, People's Republic of China; [4]Department of Cardiology, The Affiliated Cardiovascular Hospital of Qingdao University, No. 5 Zhiquan Road, Qingdao 266000, People's Republic of China; [5]Department of Radiology, The Affiliated Hospital of Qingdao University, No. 16 Jiangsu Road, Qingdao 266000, People's Republic of China; [6]Institute for Translational Medicine, The Affiliated Hospital of Qingdao University, No. 38 Dengzhou Road, Qingdao 266021, People's Republic of China

Accumulating evidence shows that tRNA-derived fragments are a novel class of functional small non-coding RNA; however, their roles in aortic dissection (AD) are still unknown. In this study, we found that 5′-tiRNA-Cys-GCA was significantly downregulated in human and mouse models of aortic dissection. The abnormal proliferation, migration, and phenotypic transition of vascular smooth muscle cells (VSMCs) played a crucial role in the initiation and progression of aortic dissection, with 5′-tiRNA-Cys-GCA as a potential phenotypic switching regulator, because its overexpression inhibited the proliferation and migration of VSMCs and increased the expression of contractile markers. In addition, we verified that signal transducer and activator of transcription 4 (STAT4) was a direct downstream target of 5′-tiRNA-Cys-GCA. We found that the STAT4 upregulation in oxidized low-density lipoprotein (ox-LDL)-treated VSMCs, which promoted cell proliferation, migration, and phenotypic transformation, was reversed by 5′-tiRNA-Cys-GCA. Furthermore, 5′-tiRNA-Cys-GCA treatment reduced the incidence and prevented the malignant process of angiotensin II- and β-aminopropionitrile-induced AD in mice. In conclusion, our findings reveal that 5′-tiRNA-Cys-GCA is a potential regulator of the AD pathological process via the STAT4 signaling pathway, providing a novel clinical target for the development of future treatment strategies for aortic dissection.

INTRODUCTION

The definition of aortic dissection (AD) is the rupture of the aortic intima due to various reasons, causing blood from the rupture orifice to enter the aortic wall, and forming the arterial wall separation..[1,2] Eighty percent of AD patients die of dissection rupture;[3] hence, once AD occurs, the patient should be immediately hospitalized and given surgical intervention. The vascular smooth muscle cells (VSMCs), an important constituent of arterial blood vessels, are believed to play a crucial role in the onset and progression of AD.[4] VSMCs have a prominent feature called phenotypic flexibility, which enables them to alternate between the contractile (differentiated) and synthetic (dedifferentiated) phenotypes.[5–8] Contractile VSMCs are characterized by the high expression of α-smooth muscle actin (α-SMA) and reduced proliferation and migration capabilities. In contrast, synthetic VSMCs contain low levels of differentiation markers and exhibit increased proliferation and migration.[9] VSMCs accelerate vascular remodeling through the occurrence of abnormal phenotypic alternations caused by various cell stimulants, such as oxidized low-density lipoprotein (ox-LDL) and platelet-derived growth factor BB (PDGF-BB).[10–12] Vascular remodeling involves the abnormal proliferation and apoptosis of VSMCs, subsequently damaging the state of vascular balance.[13,14] In addition to the abnormal proliferation and phenotypic transition of VSMCs, apoptosis is also an important link in AD progression.[15,16] Recent studies confirmed that compared with the control group, the apoptosis of VSMCs in human AD samples was more common.[17,18] Therefore, elucidation of the mechanisms involved in the phenotypic conversion and apoptosis of VSMCs during vascular remodeling under pathological conditions is essential for the development of new diagnosis and treatment strategies for AD.

The tRNA-derived stress-induced RNAs (tiRNAs) are a kind of newly discovered non-coding RNAs produced from mature tRNAs.[14,19–21] Under specific pathological conditions, mature tRNAs are cleaved by

Received 5 April 2021; accepted 17 July 2021;
https://doi.org/10.1016/j.omtn.2021.07.013.

[7]These authors contributed equally

Correspondence: Zhibin Wang, MD, Department of Cardiac Ultrasound, The Affiliated Hospital of Qingdao University, No. 16 Jiangsu Road, Qingdao 266000, People's Republic of China.
E-mail: m17853291291@163.com
Correspondence: Tao Yu, PhD, Department of Cardiac Ultrasound, The Affiliated Hospital of Qingdao University, No. 16 Jiangsu Road, Qingdao 266000, People's Republic of China.
E-mail: yutao0112@qdu.edu.cn

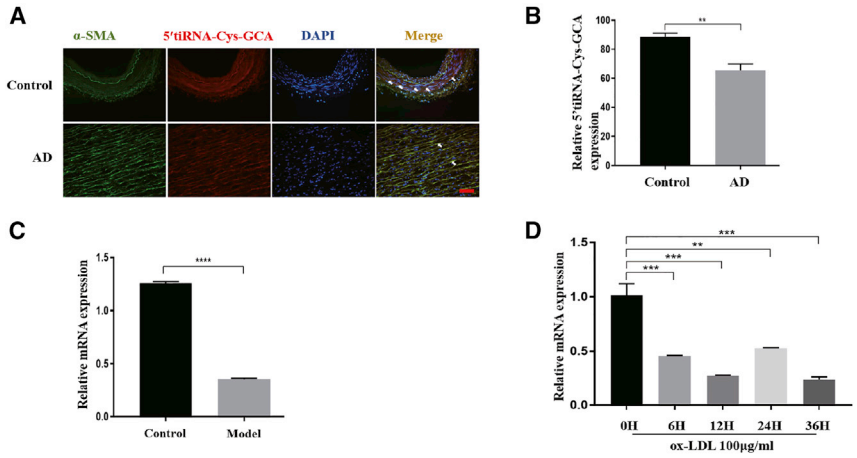

Figure 1. Differential expression and localization of 5′-tiRNA-Cys-GCA *in vivo* and *in vitro*

(A) The location of 5′-tiRNA-Cys-GCA in VSMCs was detected by FISH in human aortic and AD samples. (B) Quantification of the relative expression of 5′-tiRNA-Cys-GCA in (A). (C) Quantitative real-time PCR analysis of 5′-tiRNA-Cys-GCA expression in human aortic dissection (AD) and normal aortic tissues. (D) Quantitative real-time PCR was used to analyze 5′-tiRNA-Cys-GCA expression of VSMCs treated with ox-LDL over time gradient. Data are presented as mean ± SD. Each experiment was repeated at least three times. Scale bars, 200 μm. *$p < 0.05$; **$p < 0.01$; ***$p < 0.001$; ****$p < 0.0001$.

angiogenin (ANG), and the cleaved position in the anticodon loop will produce two kinds of tiRNAs. These two tiRNAs are 5′-tiRNAs and 3′-tiRNAs, and their length is approximately 28–36 nts.[16,22–26] Accumulating studies report that tiRNAs, which may have potential biological functions, are abnormally expressed or participate in the regulation of certain diseases, such as cancer, neurological, metabolic, and viral infectious diseases.[26–30] Notably, recent studies reveal that 5′-tiRNA is involved in regulating the proliferation and migration of cancer cells[31] and that 5′-tiRNA-Cys-GCA may be a biomarker of ischemia-reperfusion cell damage and death.[32] However, the relationship between 5′-tiRNA and cardiovascular diseases and whether 5′-tiRNA-Cys-GCA participate in the regulation of AD by altering the VSMC functions, such as proliferation and migration, are still unknown.

Signal transducer and activator of transcription 4 (STAT4) is a member of the STAT family.[33] The STAT protein is an important transcription factor located on cell surfaces.[34] After phosphorylation by JAK family proteins, STAT proteins enter the cell nucleus, combine with gene transcripts, and regulate the transcription of genes related to cell proliferation and differentiation.[35] STAT4 is highly expressed in specific organs, including the testis, spleen, heart, brain, and thymus.[36] However, several studies reveal that STAT4 can also be detected in VSMCs and may be the main regulator of VSMC proliferation or apoptosis.[34,35] Therefore, STAT4 is hypothesized to play an important role in regulating the growth of VSMC cells.

Our study explores the potential role of 5′-tiRNA-Cys-GCA in VSMCs and AD. Our findings may shed new light on the functions of 5′-tiRNA-Cys-GCA and STAT4 and identify the regulatory pathways involved in the molecular regulation of VSMCs. Future research focused on regulating the levels of 5′-tiRNA-Cys-GCA and STAT4 in VSMCs may present a new method for the interventional treatment of AD.

RESULTS

Differential expression and localization of 5′-tiRNA-Cys-GCA *in vivo* and *in vitro*

We first detected the expression level and cell localization of 5′-tiRNA-Cys-GCA in the human aorta. In the normal aorta, 5′-tiRNA-Cys-GCA was co-localized with α-SMA, suggesting that 5′-tiRNA-Cys-GCA was most likely located in VSMCs (Figure 1A). Moreover, the 5′-tiRNA-Cys-GCA expression in the AD tissue was significantly lower than in the normal aorta (Figures 1A and 1B). Consistent with these data, the 5′-tiRNA-Cys-GCA expression in AD model mice was approximately 2.5× lower than that of control mice (Figure 1C). These findings suggest that 5′-tiRNA-Cys-GCA may serve as a protective regulator in AD. To further investigate the role of 5′-tiRNA-Cys-GCA in the regulation of VSMC function, we mimicked the pathological *in vitro* model by treating VSMCs with ox-LDL (100 μg/mL), which plays a vital role in atherosclerosis and can regulate the proliferation and migration of VSMCs.[37–43] Interestingly, after ox-LDL treatment, we found that 5′-tiRNA-Cys-GCA expression exhibited a downward trend in a time-dependent manner (Figure 1D). Together, these results indicate that 5′-tiRNA-Cys-GCA was abundantly expressed in VSMCs and with close association to AD; hence, we were interested in further studying its important regulatory role in VSMC and AD.

Overexpression of 5′-tiRNA-Cys-GCA inhibits VSMC proliferation, migration, and phenotypic conversion *in vitro*

We then synthesized and transfected 5′-tiRNA-Cys-GCA mimics into VSMCs to study the regulatory function of 5′-tiRNA-Cys-GCA. The 5′-tiRNA-Cys-GCA expression in VSMCs significantly increased 24 h after transfection (Figure 2A), indicating that the 5′-tiRNA-Cys-GCA mimics were successfully incorporated and expressed in the cells. The cell counting kit-8 (CCK-8) experiment performed under the same transfection conditions also showed that VSMC proliferation was inhibited after 5′-tiRNA-Cys-GCA overexpression (Figure 2B). The 5-ethynyl-2′-deoxyuridine (EdU) assay verified the inhibitory effect of 5′-tiRNA-Cys-GCA on the proliferation of VSMCs (Figure 2C). Moreover, 5′-tiRNA-Cys-GCA suppressed the migration ability of VSMCs, as detected both by wound healing (Figure 2D) and Transwell assays (Figure 2E). We next determined whether 5′-tiRNA-Cys-GCA was involved in the phenotypic switching of VSMCs in AD. We observed that the expression of the contractile phenotype proteins significantly increased after 5′-tiRNA-Cys-GCA overexpression (Figure 2F), specifically α-SMA, while calponin 1 (CNN1) and smooth muscle myosin heavy chain (SMHC) did not show significant changes.[9] By contrast, the apoptosis

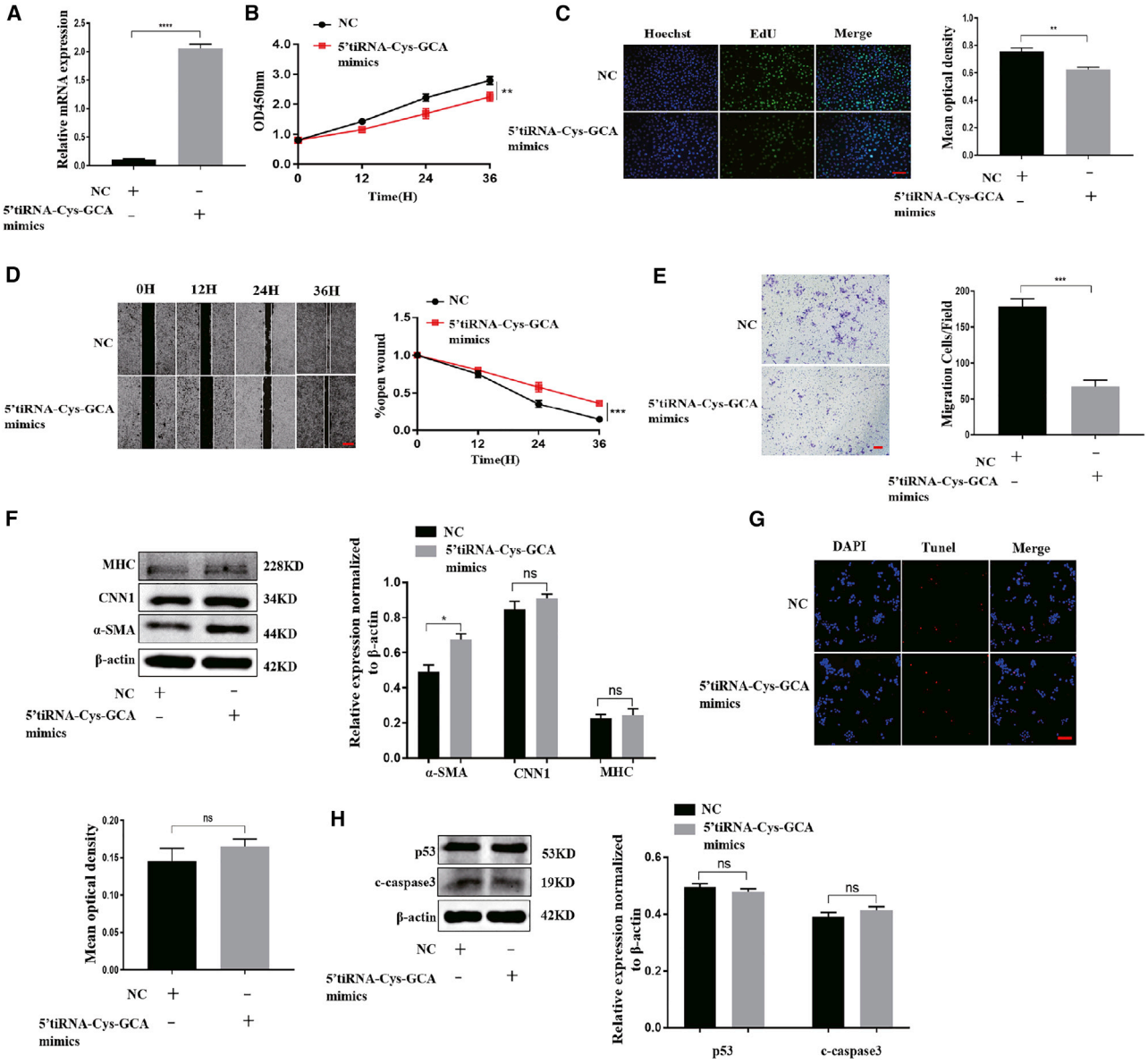

Figure 2. Overexpression of 5′-tiRNA-Cys-GCA inhibits VSMC proliferation, migration, and phenotypic conversion *in vitro*

(A) 5′-tiRNA-Cys-GCA mimics were used to overexpress 5′-tiRNA-Cys-GCA in VSMCs. The expression of 5′-tiRNA-Cys-GCA was determined using quantitative real-time PCR. (B and C) Cell counting kit-8 (CCK-8) (B) and cell-light EdU staining (C) were performed to measure cell proliferation at 0, 12, 24, and 36 h. (D and E) The cell migration after overexpression of 5′-tiRNA-Cys-GCA in VSMCs was analyzed by wound-healing (D) and Transwell (E) assay. (F) Western blotting analyses were conducted to measure the protein expression level of contractile markers after overexpression of 5′-tiRNA-Cys-GCA in VSMCs. (G and H) TUNEL assay (G) and western blot (H) were used to detect cell apoptosis after overexpression of 5′-tiRNA-Cys-GCA in VSMCs. Data are presented as mean ± SD. Each experiment was repeated at least three times. Scale bars, 200 μm. *p < 0.05; **p < 0.01; ***p < 0.001; ****p < 0.0001; ns, not significant.

rates of VSMCs did not significantly change after 5′-tiRNA-Cys-GCA overexpression (Figure 2H), which was further confirmed by detecting the expression levels of apoptosis-related proteins, p53 and cleaved caspase-3 (c-caspase-3; Figure 2G).[44,45] In summary, 5′-tiRNA-Cys-GCA mainly regulated VSMC proliferation, migration, and phenotype transition and did not significantly affect the apoptosis of VSMCs.

Knockdown of 5′-tiRNA-Cys-GCA promotes VSMC proliferation, migration, and phenotypic conversion *in vitro*

The regulatory effect of 5′-tiRNA-Cys-GCA on the proliferation, migration, and phenotypic transition of VSMCs was further verified by knockdown of 5′-tiRNA-Cys-GCA. The 5′-tiRNA-Cys-GCA expression was significantly reduced after knockdown (Figure 3A), which consequently promoted the proliferation of VSMCs (Figures

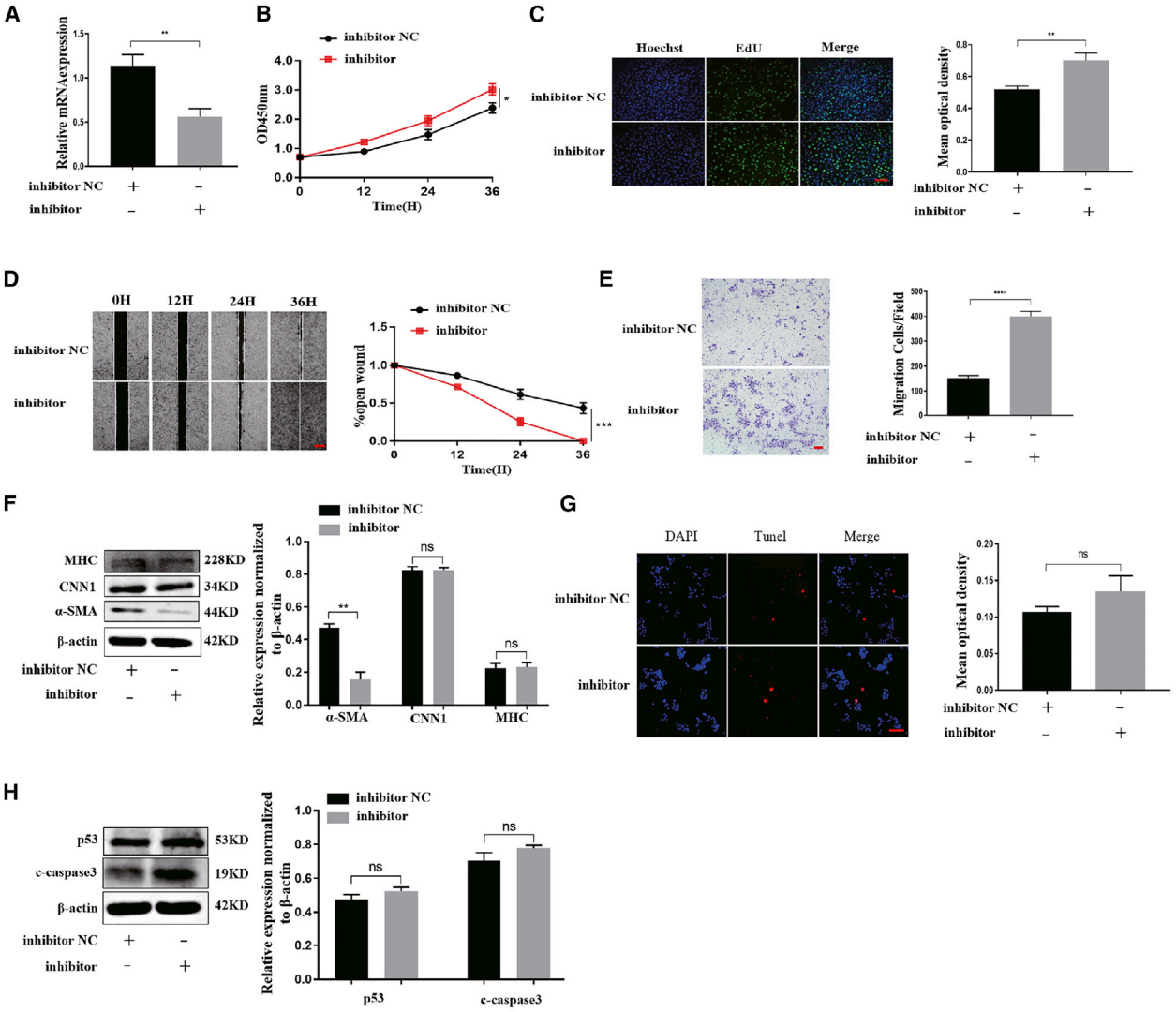

Figure 3. Knockdown of 5′-tiRNA-Cys-GCA promotes VSMC proliferation, migration, and phenotypic conversion *in vitro*

(A) 5′-tiRNA-Cys-GCA inhibitors were used to down-express 5′-tiRNA-Cys-GCA in VSMCs. The expression of 5′-tiRNA-Cys-GCA was determined using qPCR. (B and C) CCK-8 (B) and cell-light EdU staining (C) was performed to measure cell proliferation at 0, 12, 24, and 36 h. (D and E) The cell migration after down-expression of 5′-tiRNA-Cys-GCA in VSMCs was analyzed by wound-healing (D) and Transwell (E) assay. (F) Western blotting analyses were conducted to measure the protein expression level of contractile markers after down-expression of 5′-tiRNA-Cys-GCA in VSMCs. (G and H) TUNEL assay (G) and western blot (H) ware used to detect cell apoptosis after down-expression of 5′-tiRNA-Cys-GCA in VSMCs. Data are presented as mean ± SD. Each experiment was repeated at least three times. Scale bars, 200 μm. *$p < 0.05$; **$p < 0.01$; ***$p < 0.001$; ****$p < 0.0001$; ns, not significant.

3B and 3C). Simultaneously, the migration of VSMCs was significantly accelerated (Figures 3D and 3E), while the expression levels of contractile phenotype proteins were significantly reduced (Figure 3F). Furthermore, 5′-tiRNA-Cys-GCA knockdown did not produce any significant effect on VSMC apoptosis (Figures 3G and 3H). These results suggest that 5′-tiRNA-Cys-GCA knockdown promoted the proliferation, migration, and phenotypic transition of VSMCs, validating the regulatory effect of 5′-tiRNA-Cys-GCA on VSMCs.

5′-tiRNA-Cys-GCA directly binds to and downregulates STAT4

Investigation of the 5′-tiRNA-Cys-GCA-mediated regulation of VSMCs through KEGG and gene ontology (GO) analysis identified a total of 153 predicted direct downstream targets (Figure 4A). Functional analysis of the 153 predicted targets revealed that only 9 were associated with cell proliferation or migration. Furthermore, only three predicted targets, namely STAT4, PC nanoparticles (PCNP), and cysteine rich secretory protein LCCL domain containing 2 (CRISPLD2), were found to be significantly pulled down by 5′-

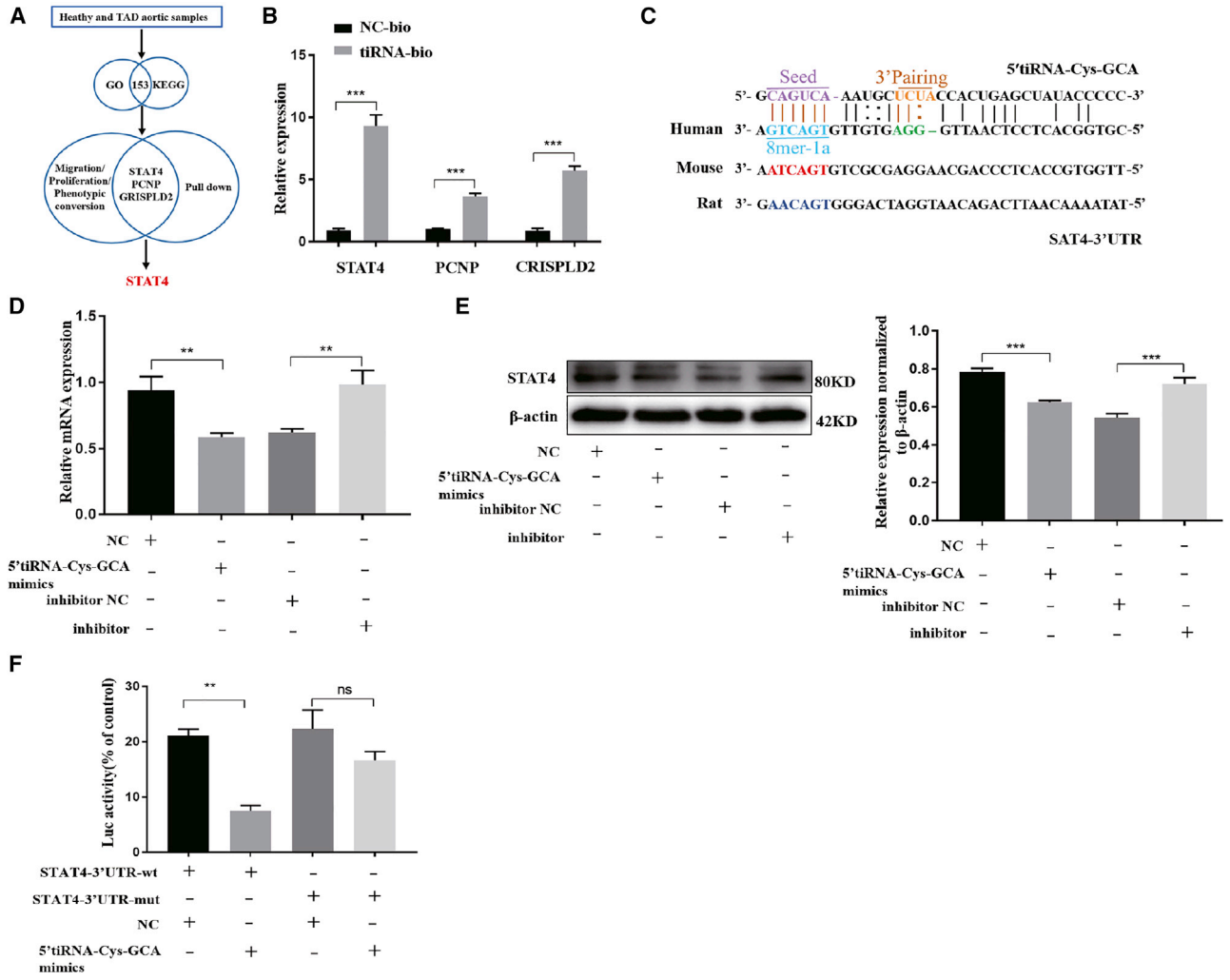

Figure 4. 5′-tiRNA-Cys-GCA directly binds to and downregulates STAT4

(A) Predicted the target genes of 5′-tiRNA-Cys-GCA by using gene ontology (GO) and kyoto encyclopaedia of genes and genomes (KEGG) enrichment analysis predictions, literature review and pull-down assay. A total of three genes were selected. (B) Pull-down assay was used to detect of the interaction between 5′-tiRNA-Cys-GCA and STAT4 in VSMCs by qPCR. (C) Theoretically predicted binding site between 5′-tiRNA-Cys-GCA and STAT4. (D and E) qPCR (D) and western blot (E) for STAT4 expression in VSMCs transfected with NC or 5′-tiRNA-Cys-GCA mimics (F) The STAT4-3′ UTR-WT or mut reporter plasmid was co-transfected into VSMCs with 5′-tiRNA-Cys-GCA mimics or NC. Luciferase activity of STAT4-3′ UTR-WT was significantly decreased by 5′-tiRNA-Cys-GCA in cells. Data are presented as mean ± SD. Each experiment was repeated at least three times. **$p < 0.01$; ***$p < 0.001$; ns, not significant.

tiRNA-Cys-GCA (Figure 4B). The quantitative PCR (qPCR) results of the remaining six targets (JAK3, KCNE3, HBEGF, TLR4, TREM1, and TNFAIP8L2) showed undetermined Ct values, indicating very low expression levels. Notably, STAT4 had the highest functional enrichment, implying that it is the most probable direct downstream target of 5′-tiRNA-Cys-GCA. Using miRanda and TargetScan software, we analyzed the predicted binding site between 5′-tiRNA-Cys-GCA and STAT4 (Figure 4C) and discovered that the structure score, free energy, and Context$^+$ values were 145, −24.79, and −0.303, respectively. Further analysis of the 5′-tiRNA-Cys-GCA and STAT4 binding displayed a high degree of conservation in humans, mice, and rats (Figure 4C). Additional experiments revealed that 5′-tiRNA-Cys-GCA overexpression inhibited the expression of STAT4 both at the mRNA (Figure 4D) and protein levels (Figure 4E), while 5′-tiRNA-Cys-GCA knockdown correspondingly increased STAT4 expression. Finally, the results of the dual luciferase reporter gene assay showed that the fluorescence intensities of the overexpressed 5′-tiRNA-Cys-GCA and transfected STAT4 wild-type luciferase reporter plasmid were significantly reduced, while there was no significant change in the mutant group. Taken together, these results suggest that 5′-tiRNA-Cys-GCA can directly bind to STAT4 and regulate its functional activities.

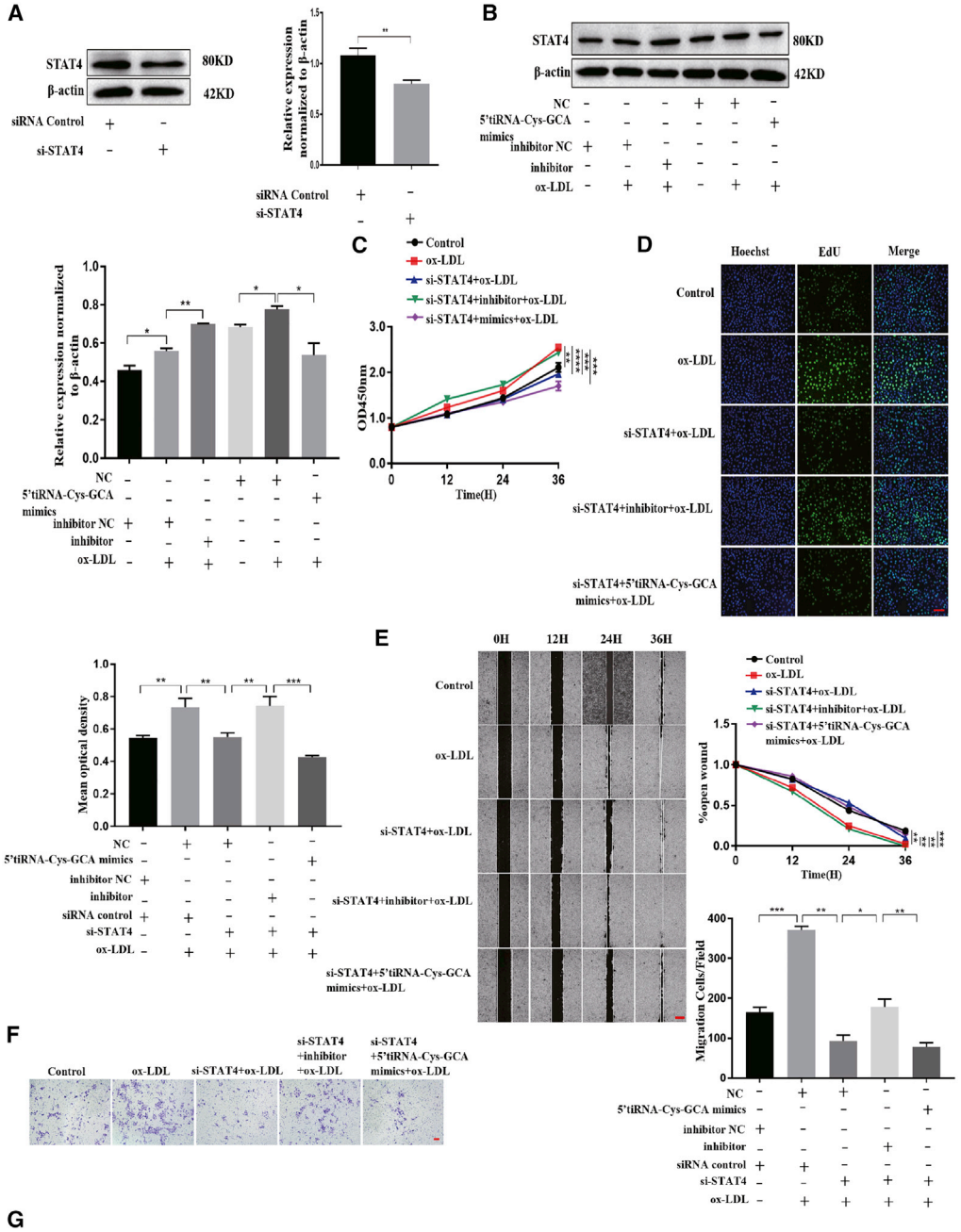

(legend on next page)

STAT4 regulates the ox-LDL-induced proliferation, migration, and phenotypic transformation of VSMCs through 5′-tiRNA-Cys-GCA

We then designed a small interfering RNA (siRNA)-mediated STAT4 knockdown experiment to further validate the regulatory effect of 5′-tiRNA-Cys-GCA on STAT4 and to study the role of the 5′-tiRNA-Cys-GCA/STAT4 axis in VSMC function and AD. First, the siRNA that specifically knocks down STAT4 (si-STAT4) was synthesized and transfected into VSMCs. The VSMCs transfected with si-STAT4 were analyzed by western blot, which showed significantly reduced STAT4 protein expression (Figure 5A). Second, since 5′-tiRNA-Cys-GCA expression exhibits a time-dependent change under ox-LDL treatment, we investigated whether STAT4 expression was also altered under ox-LDL conditions. We found that ox-LDL-treated VSMCs displayed high STAT4 expression, which was inhibited after transfection of 5′-tiRNA-Cys-GCA mimics and further promoted by 5′-tiRNA-Cys-GCA inhibitors (Figure 5B). In order to clarify the period of the regulatory effect of 5′-tiRNA-Cys-GCA on STAT4, we used inhibitors to transfect into VSMCs and then detected the expression level of STAT4. The results showed that tiRNA has the strongest regulatory effect on STAT4 within 36 h (Figure S1). Third, using 100 μg/mL ox-LDL as the pathological condition *in vitro* showed higher proliferation ability of VSMCs under ox-LDL stimulation (Figures 5C and 5D). Simultaneously, knocking down STAT4 reversed the accelerated VSMC proliferation induced by ox-LDL. Continued transfection of 5′-tiRNA-Cys-GCA mimics further reduced the proliferation of VSMCs, but transfection with the 5′-tiRNA-Cys-GCA inhibitors showed the opposite effect. Fourth, after treating the VSMCs under the same conditions, the VSMC migration was found to be consistent with the trend of VSMC proliferation determined via wound healing (Figure 5E) and Transwell assays (Figure 5F). Fifth, among the protein markers of VSMC contractile phenotype, only α-SMA had reduced expression under pathological conditions (Figure 5G); by contrast, STAT4 knockdown resulted in increased α-SMA expression. Continued transfection with 5′-tiRNA-Cys-GCA inhibitors reduced the expression level of α-SMA, while transfection with 5′-tiRNA-Cys-GCA mimics further promoted the expression of contractile phenotype proteins. In summary, knocking down STAT4 suppressed the proliferation, migration, and phenotypic switching of VSMCs, but these changes were reversed by 5′-tiRNA-Cys-GCA.

Overexpression of 5′-tiRNA-Cys-GCA reverses the AD progression in mice

To determine whether 5′-tiRNA-Cys-GCA can reverse the AD pathological process *in vivo*, we constructed AD model mice and injected 5′-tiRNA-Cys-GCA agomir through the tail veins (Figure 6). Results showed that 5′-tiRNA-Cys-GCA expression in AD model mice was significantly lower than that of the control group. However, this was reversed after the agomir injection, wherein 5′-tiRNA-Cys-GCA expression in AD model mice increased. After intraperitoneal injection of angiotensin II (AngII) and β-aminopropionitrile (BAPN) for 14 days, the AD model mice successfully developed AD. However, the dissection rupture in the injury+agomir group was found to be significantly ameliorated. In addition, slices of the aorta were stained with hematoxylin and eosin (H&E) to observe the vascular morphology. The results showed that the vascular media of the injury group was significantly thickened, but this was significantly reduced after the agomir treatment. Immunohistochemistry (IHC) analysis revealed that the STAT4 expression was significantly increased in AD tissues; however, STAT4 expression was inhibited after agomir treatment. Therefore, our findings demonstrate that we have successfully induced AD in mice to construct AD model mice. Furthermore, tiRNA treatment can reverse the pathological process of AD and thereby reduce its mortality rate, suggesting that 5′-tiRNA-Cys-GCA can potentially become a target for AD treatment.

DISCUSSION

We first investigated the function of 5′-tiRNA-Cys-GCA and discovered that 5′-tiRNA-Cys-GCA expression was significantly lower in human AD tissue compared to that of normal human aorta. Moreover, 5′-tiRNA-Cys-GCA expression showed a downward trend in VSMCs treated with ox-LDL and in the aortic tissues obtained from AD model mice. These results proved that 5′-tiRNA-Cys-GCA played a protective role in AD by regulating the function of VSMCs. Next, overexpression of 5′-tiRNA-Cys-GCA via transfection revealed that 5′-tiRNA-Cys-GCA inhibited the proliferation, migration, and phenotype switching of VSMCs, while the effects were reversed after 5′-tiRNA-Cys-GCA was knocked down. In addition to *in vitro* experiments, the 5′-tiRNA-Cys-GCA agomir treatment for AD model mice successfully reversed the AD pathological process. VSMC phenotypic transition was reported to play a very important regulatory role in the progression of AD disease; however, these reports were only based on experiments conducted under pathological conditions.[46,47] In this study, we not only discovered the differential expression of 5′-tiRNA-Cys-GCA in the human AD tissue and normal aorta but also verified that 5′-tiRNA-Cys-GCA regulates VSMC proliferation, migration, and phenotypic transition by directly binding to its downstream target, STAT4. In addition, in order to clarify whether the effect of 5′-tiRNA-Cys-GCA/STAT4 is specific in VSMCs and AD, we tested its expression level in different tissues and found that 5′-tiRNA-Cys-GCA was widely distributed in different tissues, including heart, liver, spleen, lung, kidney, aorta, brain, and skeletal muscle (Figure S2). This result indicated that the regulatory role of 5′-tiRNA-Cys-GCA may be widespread, but its expression in cardiovascular tissues is the most abundant, suggesting

Figure 5. STAT4 regulates the ox-LDL-induced proliferation, migration, and phenotypic transformation of VSMCs through 5′-tiRNA-Cys-GCA

(A–F) siRNAs were conducted to knock down STAT4 in VSMCs. (A and B) Protein level of STAT4 measured by western blot. (C and D) CCK-8 (C) and cell-light EdU staining (D) were performed to measure proliferation ability of VSMCs at 0, 12, 24, and 36 h. (E and F) The cell migration of VSMCs was analyzed by wound-healing (E) and Transwell (F) assay. (G) Western blotting analysis for the expression of contractile markers. Data are presented as mean ± SD. Each experiment was repeated at least three times. Scale bars, 200 μm. *$p < 0.05$; **$p < 0.01$; ***$p < 0.001$; ****$p < 0.0001$.

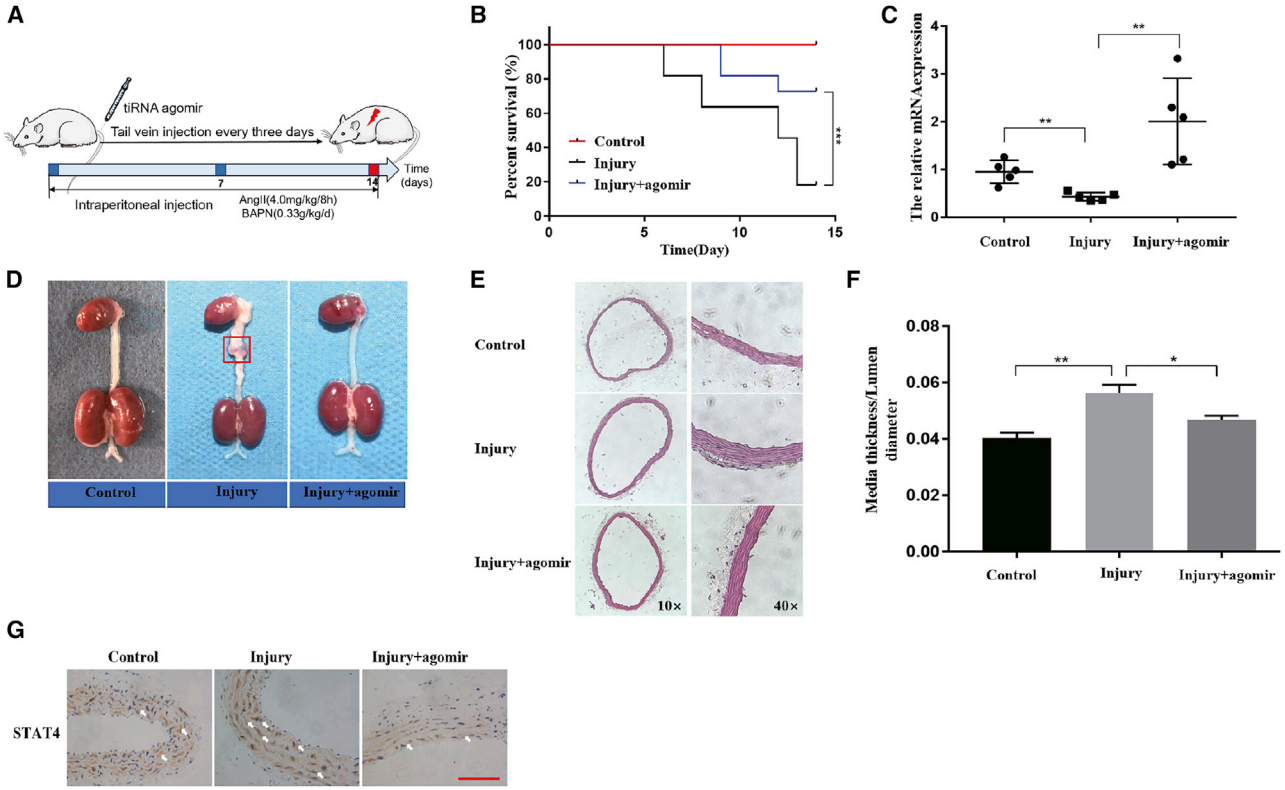

Figure 6. Overexpression of 5′-tiRNA-Cys-GCA reverses the AD progression in mice

(A) The construction of mice with AD and the tail vein injection of 5′-tiRNA-Cys-GCA agomir. (B) Survival rate curve of each group of mice. (C) qPCR was performed to detect the expression of 5′-tiRNA-Cys-GCA in thoracic arteries obtained from mice in different groups. (D) Typical images showed macroscopic features of isolated mice aorta from different groups. (E) Representative images of H&E staining in thoracic arteries obtained from mice in different groups. (F) Quantification results of media thickness/lumen diameter. (G) IHC was used to detect the expression level of STAT4 in the aorta of mice in different groups. Data are presented as mean ± SD. Each experiment was repeated at least three times. Scale bars, 200 μm. *$p < 0.05$; **$p < 0.01$; ***$p < 0.001$.

that it may play the most important roles in cardiovascular diseases. This paper is the first to report the important role of tiRNAs in cardiovascular diseases, providing new insights that may contribute to developing novel diagnosis and treatment strategies for cardiovascular diseases, especially AD.

The regulatory mechanisms of tRNA derivatives are complex and diverse. Interestingly, these tRNA derivatives had similar lengths and effects to microRNAs (miRNAs), so the mechanism by which they directly bind to the 3′ untranslated region (3′ UTR) of downstream was also called the canonical miRNAs pathway, such as 3-tRF (also called CU1276) in B cell lymphoma and tRF5-Glu in ovarian cancer.[48,49] And recent studies had also found that 5′-tiRNA^{Val} could also directly regulate downstream targets.[48] Consistently, the results of bioinformatics analysis showed that STAT4 is a potential direct downstream target of 5′-tiRNA-Cys-GCA, and it was verified by a pull-down experiment and dual luciferase reporter gene. However, we are still unable to determine whether 5′-tiRNA-Cys-GCA regulates the expression level of STAT4 by affecting the stability of STAT4, inhibiting the translation initiation complex or regulating the formation of ribosomes.[50] Then, we found that overexpression of 5′-tiRNA-Cys-GCA would cause decreased expression of STAT4 at both the mRNA and protein levels. Therefore, we speculated that 5′-tiRNA-Cys-GCA suppresses the level of STAT4 by destroying the stability of STAT4. Although previous studies found that STAT4 improves the proliferation ability of VSMCs and may become a therapeutic target for atherosclerosis,[35] there are few studies that have reported that STAT4 is involved in the phenotypic transition of VSMCs. Because STAT4 is the most prominently pulled down, we think it may be the most important downstream target in our study. However, the other two have no reports related to cardiovascular disease, but they can also be pulled down, so there may be a potential relationship with cardiovascular disease, which needs further research. Importantly, we found that knocking down STAT4 inhibits the proliferation, migration, and phenotypic transition of VSMCs induced by ox-LDL, but it was reversed after upregulation of 5′-tiRNA-Cys-GCA. In summary, 5′-tiRNA-Cys-GCA regulates the proliferation, migration, and phenotypic transition of VSMCs by directly binding downstream STAT4.

AD is a catastrophic disease and is characterized by rapid progression and high mortality.[51] At present, the main clinical treatment is to seal

the tear in the intima through surgery and reconstruct the blood flow in the area where the blood vessel is blocked due to the false cavity. However, surgical treatment is invasive and has many complications, which cannot fundamentally reduce the incidence and mortality of AD.[2] Therefore, clinicians hope to adopt conservative treatment for timely intervention in the early stage of AD and use effective drugs to prevent the recurrence of AD after surgical treatment.[2] However, exploring potential drug conservative treatment techniques is still an urgent medical problem for researchers and clinicians to solve.[52] With the continuous development of high-throughput sequencing technology, more and more small non-coding RNAs have been discovered.[53] Among them, tiRNAs are found to be derived from tRNAs and are abnormally expressed under pathological conditions. Moreover, tiRNA has important characteristics to become a diagnostic marker. The first is that tiRNAs have nucleotide modifications to further improve their stability, such as 5-methylcytidine (m5C) and 2-methylguanosine (m2G).[54] The second is that tiRNAs have high expression levels and are widely distributed in the body.[55] The third is that tiRNAs are highly conserved in vertebrates.[28] The fourth is that tiRNAs are time-specific and tissue-specific.[28] Coincidentally, the 5′-tiRNA-Cys-GCA in our study is not only abundantly expressed in normal AD tissues, but also highly conserved in humans, mice, and rats. Therefore, its differential expression is expected to become an early diagnostic biomarker of aortic dissection. Moreover, recent studies have shown that the expression level of tiRNAs is abnormal in some diseases, such as cancer, metabolic diseases, neurological diseases, and viral infection diseases.[50] Our study revealed that 5′-tiRNA-Cys-GCA bound to the direct target STAT4 to prevent the malignant proliferation, migration, and phenotype transition of VSMCs. And the 5′-tiRNA-Cys-GCA treatment in mice with AD can significantly reduce the death caused by dissection rupture and can reverse vascular remodeling. All this evidence indicates that the potential of tiRNAs is not limited to diagnostic biomarkers but is more likely to become therapeutic targets for AD.

In conclusion, the decreased expression level of 5′-tiRNA-Cys-GCA in human AD tissue suggested that it plays a protective role in the pathological process of AD. Moreover, our research showed for the first time that 5′-tiRNA-Cys-GCA acts as a regulator of phenotypic transition by targeting the STAT4 pathway, that is, preventing VSMC proliferation, migration, and phenotypic transition, as well as the progression of aortic dissection. Taken together, the 5′-tiRNA-Cys-GCA/STAT4 signaling pathway may provide a new treatment strategy for AD and more other cardiovascular diseases.

MATERIALS AND METHODS

Cell culture and treatment

Human aortic VSMCs (HASMCs) were purchased from Qingqi Biotechnology Company (BLUEFBIO, Shanghai, China) and cultured in a humidified atmosphere at 37°C and 5% CO_2 in Dulbecco's modified Eagle's medium (GIBCO, Grand Island, NY, USA) containing 10% fetal bovine serum (FBS; ExCell Bio, Shanghai, China). HASMCs were treated with ox-LDL (100 μg/mL) for 24 or 36 h to simulate ox-LDL induced pathological conditions.

Cell transfection

The 5′-tiRNA-Cys-GCA mimics, 5′-tiRNA-Cys-GCA inhibitor, siRNA against STAT4, and corresponding negative control oligonucleotides were provided by GenePharma (Shanghai, China). When HASMCs seeded into 6-well plates reached a 70%–80% confluence, they were transfected with these oligonucleotides using Lipofectamine 3000 (lipo3000; Invitrogen, United States) following the manufacturer's protocol. Oligonucleotide sequences are shown in Table S1.

RNA extraction and quantitative real-time PCR

Total RNA was purified from cell and tissue samples using Trizol (Sigma, Louis, MO, USA) following the manufacturer's instructions, Then, cDNA was synthesized using a reverse transcriptase kit (Takara, Kyoto, Japan). Quantitative real-time PCR was used to measure the RNA expression level using the SYBR Green PCR Master Mix (Yeasen, Shanghai, China). The U6 and GAPDH housekeeping genes were used to normalize the gene expression levels of target genes. Primer sequences are listed in Table S2.

Western blot

The transfected cells were placed on ice and washed with 1× PBS three times, and then protein lysis buffer was added (Solarbio, Beijing, China) to lyse the cells for 15 min. The supernatant was collected for protein quantification according to the manufacturer's instructions (Solarbio, Beijing, China), loading buffer was added to the protein, and the mixture was heated at 98°C for 10 min. The protein was separated using a 12.5% SDS-page gel and transferred to a 0.45 μm polyvinylidene fluoride (PVDF) membrane. Then, the membrane was blocked with 5% milk in tris buffer solution of tween-20 (TBST) at room temperature for 1 h. The primary antibody was diluted with 5% BSA in TBST and incubated with the membrane overnight at 4°C. The corresponding secondary antibody was also diluted with 5% BSA in TBST and incubated at room temperature for 1 h. The image was acquired using a chemiluminescence method (ProteinSimple, CA, USA) and ImageJ1.5.2 was used for quantitative analysis. The following are the dilution ratios of the primary and secondary antibodies used: rabbit anti-α-SMA (Abcam, 1:2,000), rabbit anti-CNN1 (Abcam, 1:2,000), rabbit anti-MHC (Abcam, 1:2,000), rabbit anti-STAT4 (Affinity, 1:1,000), rabbit anti-p53 (absin, 1:1,000), rabbit anti-cleaved-caspase3 (absin, 1:1,000), rabbit anti-ACTB mAb (ABclonal, 1:100,000), and goat anti-rabbit immunoglobulin G horseradish peroxidase (IgG-HRP; absin, 1:2,000).

Cell proliferation assay

Following cell transfection in a 96-well for 24 h, 10 μL CCK-8 reagent (Yeasen, Shanghai, China) was added into each well and incubated for 1 h in a 37°C incubator. Finally, a microplate reader (Thermo Fisher Scientific, Milan, Italy) was used to measure the absorbance at 450 nm.

Cell proliferation was detected using a EdU Cell Proliferation Kit (RiboBio, Guangzhou, China) following the manufacturer's protocol. Cells were incubated with 50 mM EDU solution at 37°C for 2 h, stained with Apollo Dye reaction and Hoechst stain, and then fixed

with 4% paraformaldehyde. Finally, cells were observed and imaged using a fluorescence microscope (Olympus, Tokyo, Japan).

Wound healing assay

After the cells were seeded in a 6-well plate and transfected for 24 h, 200 μL plastic tips were used to scrape the cell monolayer to form a wound, and DMEM containing 2% FBS was used for cell culture. Representative pictures were taken using an inverted phase contrast microscope at 0, 12, 24, and 36 h. The wound area at each time point was normalized to that of 0 h to assess the wound healing ability.

Transwell assay

Cells were seeded in a 12-well plate until cell confluence reached 70%–80% and transfected with target genes or control for 24 h. Then, the cells were digested with trypsin and 3×10^4 cells were respectively seeded into each 0.8-μm pore Transwell upper chamber (24-well plate, Corning, USA). A total of 200 μL DMEM without FBS was added into the upper chamber, and 500 μL DMED with 10% FBS into the lower chamber. After 24 h of migration, the cells were fixed with 4% paraformaldehyde for 0.5 h and then stained with 0.1% crystal violet for 0.5 h. Finally, 5 fields in each membrane were imaged and counted under a microscope.

Fluorescence *in situ* hybridization (FISH)

The Cy3-labeled 5′-tiRNA-Cys-GCA probe was provided by GenePharma. The human 5′-tiRNA-Cys-GCA probe sequence is 5′-GGGGGTATAGCTCAGTGGTAGAGCATTTGACTGC-3′. First, frozen slides were placed in a hypotonic KCl solution and incubated in a constant temperature water bath at 37°C for 40 min. Then, 4% paraformaldehyde was used to fix the tissue. In the dark, the probe buffer was dripped on the tissue and denatured in a wet box at 75°C for 7 min, and then the slides were placed in a wet box at 40°C for hybridization overnight. The next day, 0.4 × saline sodium citrate (SSC) and 1 × PBS were used to wash the slides, which were then stained with DAPI for 20 min. Finally, images were taken using a confocal laser microscope (Olympus, Tokyo, Japan).

RNA pull-down assay

An RNA pull-down assay was performed to verify that STAT4 is a downstream target directly bound by 5′-tiRNA-Cys-GCA, as predicted using kyoto encyclopaedia of genes and genomes (KEGG) and GO analysis. The biotinylated 5′-tiRNA-Cys-GCA was synthesized by BGI (BGI Gene, Shenzhen, China), and its sequence is 5′-GGGGGTATAGCTCAGTGGTAGAGCATTTGACTGC-3′. First, a lysis buffer was used to lyse normally cultured cells. Then, the biotinylated RNA and the blocked streptavidin agarose resin (Thermo Fisher Scientific, Milan, Italy) were incubated for 2 h at 4°C to form probe-bound beads. Next, the mixed beads were added into the cell lysate and incubated overnight at 4°C. The next day, the lysis buffer was used to elute the RNA complexes on the beads and then the Trizol-purified products (Sigma, Louis, MO, USA) were analyzed using qPCR.

IHC

Paraffin sections were deparaffinized with xylene and boiled for antigen retrieval. Then, they were incubated with hydrogen peroxide block for 10–15 min to reduce non-specific background staining caused by endogenous peroxidase. The tissues were covered with STAT4 primary antibody (Affinity, 1:200) working solution and incubated overnight at 4°C. The next day, the sections were covered with the anti-rabbit IHC antibody (ZSGB-BIO, Beijing, China) and incubated for 30 min at room temperature. Then, the tissues were stained with hematoxylin and DAB. Finally, they were mounted with a cover glass and observed and photographed under a microscope.

TUNEL assay

Cells were cultured in 24-well plates and transfected for 24 h. First, after the cells were fixed with 4% paraformaldehyde for 30 min, 0.5% Triton X-100 was used to permeabilize the cells. Then, according to the instructions of the TUNEL Apoptosis Assay Kit (MeilunBio, Dalian, China), the prepared TUNEL solution was dripped onto the cells and incubated at 37°C for 1 h. Finally, anti-fluorescence decay mounting tablets were used to mount the slides. The results were observed using a fluorescence microscope and images were obtained in 5 fields of view.

Dual luciferase reporter assay

The binding sites of 5′-tiRNA-Cys-GCA and STAT4 were identified through the TargetScan database. The STAT4 wild-type (STAT4-WT) and mutant (STAT4-MUT) luciferase reporter plasmids were designed and synthesized by TSINGKE Biology Technology (Qingdao, China). The cells were cultured in 24-well plates, and then lipo3000 was used to transfect the luciferase reporter vector and 5′-tiRNA-Cys-GCA mimic or 5′-tiRNA-Cys-GCA negative control (NC) into HASMCs. 24 h after transfection, Nano&Firefly-Glo Luciferase Reporter Assay Kit (MeilunBio, Dalian, China) was used to detect relative luciferase activity.

Histological analysis

The mouse thoracic aortas were collected and cut into 8 μm frozen sections. A H&E staining kit (MeilunBio, Dalian, China) was used to stain the tissue according to the manufacturer's instructions. Finally, the tissue condition was observed using an optical microscope. ImageJ was used to measure the media thickness and vessel lumen diameter.

Collection of AD tissue and AD murine model

The AD tissues were obtained from patients undergoing aortic resection in the Affiliated Hospital of Qingdao University, and the normal aortas were collected from the adjacent tissue of the gastrointestinal tumor in patients. The tissues were stored in liquid nitrogen for the experiments in this study. The Affiliated Hospital of Qingdao University approved the study, and the patients signed an informed consent form.

The 3-week-old male FVB mice were provided by Vital River Laboratory Animal Technology (Beijing, China). All mice were bred

in the animal room of the Institute of Translational Medicine of Qingdao University. They were given 12 h of light every day and had a regular diet and weighed every 3 days. The mice were divided into 3 groups (control group, injury group, injury + agomir group), with 11 mice in each group. Among them, the injury group and the injury + agomir group were used to construct the AD model; that is, intraperitoneal injection of AngII (GL Biochem, Shanghai, China) 4.0 mg/kg/8 h combined with intraperitoneal injection of BAPN (Aladdin, Shanghai, China) 0.33 g/kg/d for 14 days, while mice in the control group were injected intraperitoneally with the same amount of saline. At the same time, mice in the injury + agomir group were injected with 5′-tiRNA-Cys-GCA agomir (0.625 mg/kg) through the tail vein.[56] 5′-tiRNA-Cys-GCA agomir was designed and synthesized by Sangon Biotech (Shanghai, China; sense: 5′-GCAGUCAAAUGCUCUAC CACUGAGCUAUACCCCCC-3′; antisense: 5′-GGGUAUAGCUCA GUGGUAGAGCAUUUGACUGCUU-3′). Agomir was transfected *in vivo* with a plasmid/PEI/PEG cocktail twice a week.[40,57] The dead mice were dissected directly and the aorta was taken out. The mice were sacrificed 14 days later, and the aorta was taken out for pathological observation and RNA extraction. All animal experiment operations were approved by the Animal Ethics Committee of the Affiliated Hospital of Qingdao University (Shandong, China) and were carried out in accordance with the requirements.

Statistical analysis

All data were shown as mean ± SD and analyzed by GraphPad Prism 7.0. The analysis between the data uses unpaired t test, ANOVA with Tukey post-hoc tests. $p < 0.05$ is considered to be significant. All experimental results are obtained from at least three replicates.

SUPPLEMENTAL INFORMATION

Supplemental information can be found online at https://doi.org/10.1016/j.omtn.2021.07.013.

ACKNOWLEDGMENTS

This work was supported by The National Natural Science Foundation of China (grant number 81870331), The Natural Science Foundation of Shandong Province (grant number ZR2020MH045), The Qingdao municipal science and technology bureau project (grant number 21-1-4-rkjk-12-nsh), and Qingdao University Medical Group Project (YLJT20201012).

AUTHOR CONTRIBUTIONS

T.Z., Y.Y., T.Y., and Z.W. designed and conducted this experiment. T.Z. wrote the manuscript and prepared tables and figures. T.Z. viewed and approved the manuscript. All authors read the manuscript and approved the final manuscript.

DECLARATION OF INTEREST

The authors declare no competing interests.

REFERENCES

1. Sun, Y., Xiao, Y., Sun, H., Zhao, Z., Zhu, J., Zhang, L., Dong, J., Han, T., Jing, Q., Zhou, J., and Jing, Z. (2019). miR-27a regulates vascular remodeling by targeting endothelial cells' apoptosis and interaction with vascular smooth muscle cells in aortic dissection. Theranostics *9*, 7961–7975.
2. Cheng, M., Yang, Y., Xin, H., Li, M., Zong, T., He, X., Yu, T., and Xin, H. (2020). Non-coding RNAs in aortic dissection: From biomarkers to therapeutic targets. J. Cell. Mol. Med. *24*, 11622–11637.
3. Thompson, R.W. (2002). Detection and management of small aortic aneurysms. N. Engl. J. Med. *346*, 1484–1486.
4. Liu, S., Yang, Y., Jiang, S., Tang, N., Tian, J., Ponnusamy, M., Tariq, M.A., Lian, Z., Xin, H., and Yu, T. (2018). Understanding the role of non-coding RNA (ncRNA) in stent restenosis. Atherosclerosis *272*, 153–161.
5. Li, F.J., Zhang, C.L., Luo, X.J., Peng, J., and Yang, T.L. (2019). Involvement of the MiR-181b-5p/HMGB1 Pathway in Ang II-induced Phenotypic Transformation of Smooth Muscle Cells in Hypertension. Aging Dis. *10*, 231–248.
6. Wang, Y., Dong, C.Q., Peng, G.Y., Huang, H.Y., Yu, Y.S., Ji, Z.C., and Shen, Z.Y. (2019). MicroRNA-134-5p Regulates Media Degeneration through Inhibiting VSMC Phenotypic Switch and Migration in Thoracic Aortic Dissection. Mol. Ther. Nucleic Acids *16*, 284–294.
7. Davis-Dusenbery, B.N., Wu, C., and Hata, A. (2011). Micromanaging vascular smooth muscle cell differentiation and phenotypic modulation. Arterioscler. Thromb. Vasc. Biol. *31*, 2370–2377.
8. Fu, X., Zong, T., Yang, P., Li, L., Wang, S., Wang, Z., Li, M., Li, X., Zou, Y., Zhang, Y., et al. (2021). Nicotine: Regulatory roles and mechanisms in atherosclerosis progression. Food Chem. Toxicol. *151*, 112154.
9. Owens, G.K., Kumar, M.S., and Wamhoff, B.R. (2004). Molecular regulation of vascular smooth muscle cell differentiation in development and disease. Physiol. Rev. *84*, 767–801.
10. Inamoto, S., Kwartler, C.S., Lafont, A.L., Liang, Y.Y., Fadulu, V.T., Duraisamy, S., Willing, M., Estrera, A., Safi, H., Hannibal, M.C., et al. (2010). TGFBR2 mutations alter smooth muscle cell phenotype and predispose to thoracic aortic aneurysms and dissections. Cardiovasc. Res. *88*, 520–529.
11. Jones, J.A., Beck, C., Barbour, J.R., Zavadzkas, J.A., Mukherjee, R., Spinale, F.G., and Ikonomidis, J.S. (2009). Alterations in aortic cellular constituents during thoracic aortic aneurysm development: myofibroblast-mediated vascular remodeling. Am. J. Pathol. *175*, 1746–1756.
12. Wang, X., Li, H., Zhang, Y., Liu, Q., Sun, X., He, X., Yang, Q., Yuan, P., and Zhou, X. (2021). Suppression of miR-4463 promotes phenotypic switching in VSMCs treated with Ox-LDL. Cell Tissue Res. *383*, 1155–1165.
13. McMurtry, M.S., Bonnet, S., Wu, X., Dyck, J.R., Haromy, A., Hashimoto, K., and Michelakis, E.D. (2004). Dichloroacetate prevents and reverses pulmonary hypertension by inducing pulmonary artery smooth muscle cell apoptosis. Circ. Res. *95*, 830–840.
14. Yang, X., Yang, Y., Guo, J., Meng, Y., Li, M., Yang, P., Liu, X., Aung, L.H.H., Yu, T., and Li, Y. (2021). Targeting the epigenome in in-stent restenosis: from mechanisms to therapy. Mol. Ther. Nucleic Acids *23*, 1136–1160.
15. Liao, W.L., Tan, M.W., Yuan, Y., Wang, G.K., Wang, C., Tang, H., and Xu, Z.Y. (2015). Brahma-related gene 1 inhibits proliferation and migration of human aortic smooth muscle cells by directly up-regulating Ras-related associated with diabetes in the pathophysiologic processes of aortic dissection. J. Thorac. Cardiovasc. Surg. *150*, 1292–301.e2.
16. Wang, L., Zhang, J., Fu, W., Guo, D., Jiang, J., and Wang, Y. (2012). Association of smooth muscle cell phenotypes with extracellular matrix disorders in thoracic aortic dissection. J Vasc Surg. *56*, 1698–1709.
17. Xiao, Y., Sun, Y., Ma, X., Wang, C., Zhang, L., Wang, J., Wang, G., Li, Z., Tian, W., Zhao, Z., et al. (2020). MicroRNA-22 Inhibits the Apoptosis of Vascular Smooth Muscle Cell by Targeting p38MAPKα in Vascular Remodeling of Aortic Dissection. Mol. Ther. Nucleic Acids *22*, 1051–1062.
18. Shi, Y., Liu, B., Wang, C.S., and Yang, C.S. (2018). MST1 down-regulation in decreasing apoptosis of aortic dissection smooth muscle cell apoptosis. Eur. Rev. Med. Pharmacol. Sci. *22*, 2044–2051.
19. Li, S., Xu, Z., and Sheng, J. (2018). tRNA-Derived Small RNA: A Novel Regulatory Small Non-Coding RNA. Genes (Basel) *9*, 246.

20. Li, M., Yang, Y., Wang, Z., Zong, T., Fu, X., Aung, L.H.H., Wang, K., Wang, J.X., and Yu, T. (2021). Piwi-interacting RNAs (piRNAs) as potential biomarkers and therapeutic targets for cardiovascular diseases. Angiogenesis *24*, 19–34.

21. Yang, Y., Yu, T., Jiang, S., Zhang, Y., Li, M., Tang, N., Ponnusamy, M., Wang, J.X., and Li, P.F. (2017). miRNAs as potential therapeutic targets and diagnostic biomarkers for cardiovascular disease with a particular focus on WO2010091204. Expert Opin. Ther. Pat. *27*, 1021–1029.

22. Saikia, M., Krokowski, D., Guan, B.J., Ivanov, P., Parisien, M., Hu, G.F., Anderson, P., Pan, T., and Hatzoglou, M. (2012). Genome-wide identification and quantitative analysis of cleaved tRNA fragments induced by cellular stress. J. Biol. Chem. *287*, 42708–42725.

23. Yamasaki, S., Ivanov, P., Hu, G.F., and Anderson, P. (2009). Angiogenin cleaves tRNA and promotes stress-induced translational repression. J. Cell Biol. *185*, 35–42.

24. He, X., Yang, Y., Wang, Q., Wang, J., Li, S., Li, C., Zong, T., Li, X., Zhang, Y., Zou, Y., and Yu, T. (2021). Expression profiles and potential roles of transfer RNA-derived small RNAs in atherosclerosis. J. Cell. Mol. Med. *25*, 7052–7065.

25. Zhang, Y., Yang, Y., He, X., Yang, P., Zong, T., Sun, P., Sun, R.C., Yu, T., and Jiang, Z. (2021). The cellular function and molecular mechanism of formaldehyde in cardiovascular disease and heart development. J. Cell. Mol. Med. *25*, 5358–5371.

26. Yang, L., Han, D., Zhan, Q., Li, X., Shan, P., Hu, Y., Ding, H., Wang, Y., Zhang, L., Zhang, Y., et al. (2019). Blood TfR+ exosomes separated by a pH-responsive method deliver chemotherapeutics for tumor therapy. Theranostics *9*, 7680–7696.

27. Shen, Y., Yu, X., Zhu, L., Li, T., Yan, Z., and Guo, J. (2018). Transfer RNA-derived fragments and tRNA halves: biogenesis, biological functions and their roles in diseases. J. Mol. Med. (Berl.) *96*, 1167–1176.

28. Zhang, Y., Zhang, Y., Shi, J., Zhang, H., Cao, Z., Gao, X., Ren, W., Ning, Y., Ning, L., Cao, Y., et al. (2014). Identification and characterization of an ancient class of small RNAs enriched in serum associating with active infection. J. Mol. Cell Biol. *6*, 172–174.

29. Qi, H., Wang, Y., Yuan, X., Li, P., and Yang, L. (2020). Selective extracellular arginine deprivation by a single injection of cellular non-uptake arginine deiminase nanocapsules for sustained tumor inhibition. Nanoscale *12*, 24030–24043.

30. Qi, H., Yang, L., Shan, P., Zhu, S., Ding, H., Xue, S., Wang, Y., Yuan, X., and Li, P. (2020). The Stability Maintenance of Protein Drugs in Organic Coatings Based on Nanogels. Pharmaceutics *12*, 115.

31. Mo, D., Jiang, P., Yang, Y., Mao, X., Tan, X., Tang, X., Wei, D., Li, B., Wang, X., Tang, L., and Yan, F. (2019). A tRNA fragment, 5′-tiRNA^{Val}, suppresses the Wnt/β-catenin signaling pathway by targeting FZD3 in breast cancer. Cancer Lett. *457*, 60–73.

32. Elkordy, A., Rashad, S., Shehabeldeen, H., Mishima, E., Niizuma, K., Abe, T., and Tominaga, T. (2019). tiRNAs as a novel biomarker for cell damage assessment in in vitro ischemia-reperfusion model in rat neuronal PC12 cells. Brain Res. *1714*, 8–17.

33. Verhoeven, Y., Tilborghs, S., Jacobs, J., De Waele, J., Quatannens, D., Deben, C., Prenen, H., Pauwels, P., Trinh, X.B., Wouters, A., et al. (2020). The potential and controversy of targeting STAT family members in cancer. Semin. Cancer Biol. *60*, 41–56.

34. Lv, L., Meng, Q., Ye, M., Wang, P., and Xue, G. (2014). STAT4 deficiency protects against neointima formation following arterial injury in mice. J. Mol. Cell. Cardiol. *74*, 284–294.

35. Guo, F., Zarella, C., and Wagner, W.D. (2006). STAT4 and the proliferation of artery smooth muscle cells in atherosclerosis. Exp. Mol. Pathol. *81*, 15–22.

36. Yamamoto, K., Kobayashi, H., Arai, A., Miura, O., Hirosawa, S., and Miyasaka, N. (1997). cDNA cloning, expression and chromosome mapping of the human STAT4 gene: both STAT4 and STAT1 genes are mapped to 2q32.2–>q32.3. Cytogenet. Cell Genet. *77*, 207–210.

37. Xue, Q., He, N., Wang, Z., Fu, X., Aung, L.H.H., Liu, Y., Li, M., Cho, J.Y., Yang, Y., and Yu, T. (2021). Functional roles and mechanisms of ginsenosides from Panax ginseng in atherosclerosis. J. Ginseng Res. *45*, 22–31.

38. Tang, N., Jiang, S., Yang, Y., Liu, S., Ponnusamy, M., Xin, H., and Yu, T. (2018). Noncoding RNAs as therapeutic targets in atherosclerosis with diabetes mellitus. Cardiovasc. Ther. *36*, e12436.

39. Bai, B., Yang, Y., Wang, Q., Li, M., Tian, C., Liu, Y., Aung, L.H.H., Li, P.F., Yu, T., and Chu, X.M. (2020). NLRP3 inflammasome in endothelial dysfunction. Cell Death Dis. *11*, 776.

40. He, X., Lian, Z., Yang, Y., Wang, Z., Fu, X., Liu, Y., Li, M., Tian, J., Yu, T., and Xin, H. (2020). Long Non-coding RNA PEBP1P2 Suppresses Proliferative VSMCs Phenotypic Switching and Proliferation in Atherosclerosis. Mol. Ther. Nucleic Acids *22*, 84–98.

41. Wang, Q., Yang, Y., Fu, X., Wang, Z., Liu, Y., Li, M., Zhang, Y., Li, Y., Li, P.F., Yu, T., and Chu, X.M. (2020). Long noncoding RNA XXYLT1-AS2 regulates proliferation and adhesion by targeting the RNA binding protein FUS in HUVEC. Atherosclerosis *298*, 58–69.

42. Liu, Y., Yang, Y., Wang, Z., Fu, X., Chu, X.M., Li, Y., Wang, Q., He, X., Li, M., Wang, K., et al. (2020). Insights into the regulatory role of circRNA in angiogenesis and clinical implications. Atherosclerosis *298*, 14–26.

43. Yu, T., Wang, Z., Jie, W., Fu, X., Li, B., Xu, H., Liu, Y., Li, M., Kim, E., Yang, Y., and Cho, J.Y. (2020). The kinase inhibitor BX795 suppresses the inflammatory response via multiple kinases. Biochem. Pharmacol. *174*, 113797.

44. Du, Y., Qian, B., Gao, L., Tan, P., Chen, H., Wang, A., Zheng, T., Pu, S., Xia, X., and Fu, W. (2019). Aloin Preconditioning Attenuates Hepatic Ischemia/Reperfusion Injury via Inhibiting TLR4/MyD88/NF-κB Signal Pathway *In Vivo* and *In Vitro*. Oxid. Med. Cell. Longev. *2019*, 3765898.

45. Su, Q., Lv, X.W., Xu, Y.L., Cai, R.P., Dai, R.X., Yang, X.H., Zhao, W.K., and Kong, B.H. (2021). Exosomal LINC00174 derived from vascular endothelial cells attenuates myocardial I/R injury via p53-mediated autophagy and apoptosis. Mol. Ther. Nucleic Acids *23*, 1304–1322.

46. Zhang, J., Wang, L., Fu, W., Wang, C., Guo, D., Jiang, J., and Wang, Y. (2013). Smooth muscle cell phenotypic diversity between dissected and unaffected thoracic aortic media. J. Cardiovasc. Surg. (Torino) *54*, 511–521.

47. Liu, S., Yang, Y., Jiang, S., Xu, H., Tang, N., Lobo, A., Zhang, R., Liu, S., Yu, T., and Xin, H. (2019). MiR-378a-5p Regulates Proliferation and Migration in Vascular Smooth Muscle Cell by Targeting CDK1. Front. Genet. *10*, 22.

48. Maute, R.L., Schneider, C., Sumazin, P., Holmes, A., Califano, A., Basso, K., and Dalla-Favera, R. (2013). tRNA-derived microRNA modulates proliferation and the DNA damage response and is down-regulated in B cell lymphoma. Proc. Natl. Acad. Sci. USA *110*, 1404–1409.

49. Zhou, K., Diebel, K.W., Holy, J., Skildum, A., Odean, E., Hicks, D.A., Schotl, B., Abrahante, J.E., Spillman, M.A., and Bemis, L.T. (2017). A tRNA fragment, tRF5-Glu, regulates BCAR3 expression and proliferation in ovarian cancer cells. Oncotarget *8*, 95377–95391.

50. Zong, T., Yang, Y., Zhao, H., Li, L., Liu, M., Fu, X., Tang, G., Zhou, H., Aung, L.H.H., Li, P., et al. (2021). tsRNAs: Novel small molecules from cell function and regulatory mechanism to therapeutic targets. Cell Prolif. *54*, e12977.

51. Yu, X., Suki, B., and Zhang, Y. (2020). Avalanches and power law behavior in aortic dissection propagation. Sci. Adv. *6*, eaaz1173.

52. Yang, K., Ren, J., Li, X., Wang, Z., Xue, L., Cui, S., Sang, W., Xu, T., Zhang, J., Yu, J., et al. (2020). Prevention of aortic dissection and aneurysm via an ALDH2-mediated switch in vascular smooth muscle cell phenotype. Eur. Heart J. *41*, 2442–2453.

53. Huang, S.Q., Sun, B., Xiong, Z.P., Shu, Y., Zhou, H.H., Zhang, W., Xiong, J., and Li, Q. (2018). The dysregulation of tRNAs and tRNA derivatives in cancer. J. Exp. Clin. Cancer Res. *37*, 101.

54. Tuorto, F., Liebers, R., Musch, T., Schaefer, M., Hofmann, S., Kellner, S., Frye, M., Helm, M., Stoecklin, G., and Lyko, F. (2012). RNA cytosine methylation by Dnmt2 and NSun2 promotes tRNA stability and protein synthesis. Nat. Struct. Mol. Biol. *19*, 900–905.

55. Godoy, P.M., Bhakta, N.R., Barczak, A.J., Cakmak, H., Fisher, S., MacKenzie, T.C., Patel, T., Price, R.W., Smith, J.F., Woodruff, P.G., and Erle, D.J. (2018). Large Differences in Small RNA Composition Between Human Biofluids. Cell Rep. *25*, 1346–1358.

56. Zhou, J.N., Zeng, Q., Wang, H.Y., Zhang, B., Li, S.T., Nan, X., Cao, N., Fu, C.J., Yan, X.L., Jia, Y.L., et al. (2015). MicroRNA-125b attenuates epithelial-mesenchymal transitions and targets stem-like liver cancer cells through small mothers against decapentaplegic 2 and 4. Hepatology *62*, 801–815.

57. Sakae, M., Ito, T., Yoshihara, C., Iida-Tanaka, N., Yanagie, H., Eriguchi, M., and Koyama, Y. (2008). Highly efficient in vivo gene transfection by plasmid/PEI complexes coated by anionic PEG derivatives bearing carboxyl groups and RGD peptide. Biomed. Pharmacother. *62*, 448–453.